INSTITUTE OF PHYSICS PUBLISHING CLASSICAL AND QUANTUM GRAVITY

Class. Quantum Grav. **18** (2001) 3473–3495 PII: S0264-9381(01)23520-5

Space missions to detect the cosmic gravitational-wave background

Neil J Cornish[1] **and Shane L Larson**

Department of Physics, Montana State University, Bozeman, MT 59717, USA

E-mail: cornish@physics.montana.edu

Received 2 April 2001, in final form 18 May 2001
Published 14 August 2001
Online at stacks.iop.org/CQG/18/3473

Abstract

It is thought that a stochastic background of gravitational waves was produced during the formation of the universe. A great deal could be learned by measuring this cosmic gravitational-wave background (CGB), but detecting the CGB presents a significant technological challenge. The signal strength is expected to be extremely weak, and there will be competition from unresolved astrophysical foregrounds such as white dwarf binaries. Our goal is to identify the most promising approach to detecting the CGB. We study the sensitivities that can be reached using both individual, and cross-correlated pairs of space-based interferometers. Our main result is a general, coordinate-free formalism for calculating the detector response that applies to arbitrary detector configurations. We use this general formalism to identify some promising designs for a gravitational background interferometer mission. Our conclusion is that detecting the CGB may not be out of reach.

PACS numbers: 9870, 9880

(Some figures in this article are in colour only in the electronic version)

1. Introduction

Before embarking on a quest to discover the cosmic gravitational-wave background (CGB), it is worth reflecting on how much has been learned from its electromagnetic analogue, the cosmic microwave background (CMB). The recent Boomerang [1] and Maxima [2] experiments have furnished detailed pictures of the universe some 300 000 yr after the big bang. These measurements of the CMB anisotropies have been used to infer that the visible universe is, to a good approximation, spatially flat. The earlier COBE-DMR [3] measurements of the CMB anisotropy fixed the scale for the density perturbations that formed the large-scale structure

[1] Author to whom correspondence should be addressed.

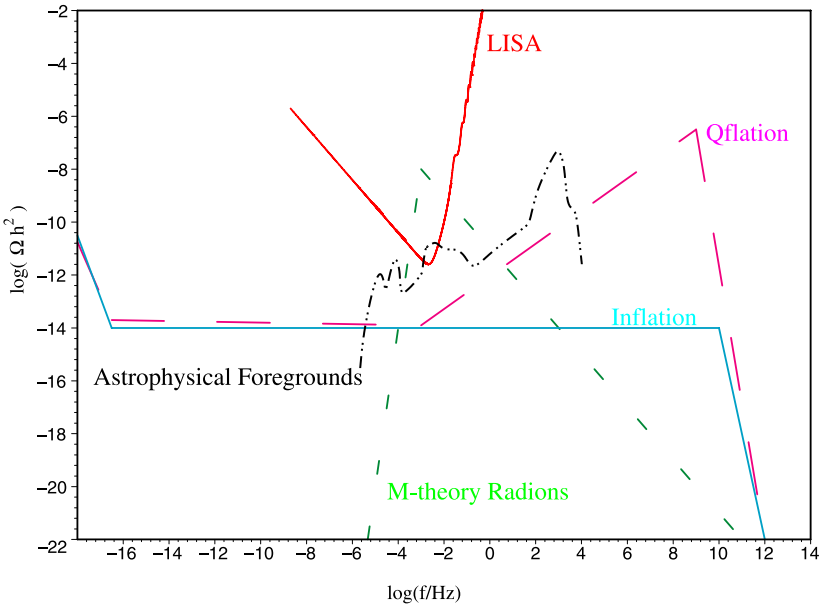

Figure 1. Possible sources of a stochastic gravitational-wave background plotted against the sensitivity curve for the LISA mission.

we see today, and showed that the density perturbations have an almost scale-free spectrum. With all this excitement over the anisotropy measurements it is easy to forget how much the CMB taught us before the anisotropies were detected. The initial observation that the CMB is highly *isotropic* is one of the major observational triumphs of the big-bang theory. Equally important was the discovery by COBE-FIRAS [4] that the CMB has an exquisite black-body spectrum with a temperature of 2.728 K.

The lesson that we take from the CMB is that while it would be wonderful to have a COBE-style map of the early universe in gravitational waves, a great deal can be learned by detecting the isotropic component. The main focus of this work is on the fixing the amplitude of the CGB at some frequency. Some attention will also be given to the prospects of measuring the energy spectrum. Detecting anisotropies in the CGB is a considerably harder problem that we address elsewhere [5].

There are two major obstacles that stand in the way of detecting the CGB. The first is the extreme weakness of the signal, and the second is the competing stochastic background produced by astrophysical sources. Figure 1 shows various predictions for the CGB energy spectra in several early-universe scenarios including standard inflation, a particular M-theory model [6] and quintessence-based inflation [7]. Also shown is the sensitivity curve for the proposed Laser Interferometer Space Antenna (LISA) [8], and a compilation of possible extragalactic astrophysical foregrounds taken from the work of Schneider *et al* [9]. Starting from low frequencies and working up, the extragalactic foreground is dominated by black hole–black hole binaries, white dwarf–white dwarf binaries, population III stars, neutron star–neutron star binaries, r-modes of neutron stars and supernova core collapse. The spectrum is expressed in terms of $\Omega_{\rm gw}(f)h_o^2$, the energy density in gravitational waves (in units of the critical density) per logarithmic frequency interval,

$$\Omega_{\rm gw}(f) = \frac{1}{\rho_c}\frac{{\rm d}\rho\,(f)}{{\rm d}\ln f}, \tag{1}$$

multiplied by h_0^2, where h_0 is the Hubble constant in units of 100 km s^{-1} Mpc^{-1}. The predictions for the CGB power spectra are fairly optimistic, and some of them are close to saturating existing indirect bounds on $\Omega_{\rm gw}(f)$ (see the review by Maggiore for details [10]). For example, data from the Cosmic Background Explorer (COBE) can be used to produce the bound $\Omega_{\rm gw}(f)h_o^2 < 2.6 \times 10^{-14}$ [11] for scale-invariant inflationary models.

With the exception of the M-theory motivated model, we see that the major obstacle to detecting the CGB is not the sensitivity of our detectors, but competition from astrophysical foregrounds. The astrophysical foregrounds are produced by the combination of a great number of weak sources that add together to form a significant stochastic signal. Based on current estimates, it is thought that the contribution from astrophysical sources falls off fairly rapidly below 1 μHz. For that reason, we will focus our attention on detecting the CGB in the sub-microhertz regime. To put this number into perspective, an interferometer built using LISA technology would need spacecraft separated by one-tenth of a light year to reach a peak sensitivity at 1 μHz! A more practical approach is to use two smaller interferometers that lack the intrinsic sensitivity to detect the CGB on their own, but together are able to reach the required sensitivity. The idea is to cross-correlate the outputs from the two interferometers and integrate over some long observation time T. Since the noise in the two interferometers is uncorrelated while the signal is correlated, the signal-to-noise ratio will steadily improve as the observation time is increased.

In principle, it is possible to detect an arbitrarily weak signal by observing for an arbitrarily long time. In practice, the prospects are not so rosy as the sensitivity of the detector pair only improves on the sensitivity of a single detector as $(T\Delta f)^{1/2}$, where Δf is the frequency bandpass. The frequency bandpass is typically taken to equal the central observing frequency. Suppose we try and look for the CGB at a frequency of $f \approx \Delta f = 10^3$ Hz using the two LIGO detectors. Over an observation time of $T = 1$ yr, the sensitivity is improved by a factor of $\sim 2 \times 10^5$ by cross-correlating the Washington and Louisiana detectors. For a pair of LISA detectors with a bandpass of $\Delta f \approx 10^{-2}$ Hz, cross-correlating for a year would result in a 500-fold improvement in sensitivity. However, for detectors operating in the μHz range, cross-correlating two detectors for 1 yr only improves on the sensitivity of a single detector by a factor of ~ 6. So why use two interferometers when one will do? The reason is simple: with a single interferometer it is not possible to tell the difference between the CGB and instrument noise since both are, to a good approximation, stationary Gaussian random processes. Moreover, it is impossible to shield a detector from gravitational waves in order to establish the noise floor. With two or more independent interferometers the cross-correlated signal can be used to separate the stochastic background from instrument noise. The LISA system has three arms, and the signal from these arms can be used to form three different Michelson interferometers. However, these interferometers share spacecraft, and thus common sources of noise, so nothing is gained by cross-correlating the outputs. Tinto *et al* [12] have recently suggested another way of combining the signals, known as a Sagnac system, which creates an interferometer that is fairly insensitive to gravitational waves. The Sagnac signal is formed by differencing signals that are sent clockwise and counter-clockwise around the triangle formed by the three LISA spacecraft. The response of this Sagnac interferometer is noise dominated at low frequencies, so its output can be used to estimate the low-frequency noise floor for the standard interferometer configuration. Thus, a single LISA-type observatory might be able to discriminate between the CGB and instrument noise [13].

We will show that cross-correlating two LISA interferometers results in a signal-to-noise ratio of

$$\mathrm{SNR} = 1.44 \left(\frac{T}{\mathrm{yr}}\right)^{1/2} \left(\frac{\Omega_{\rm gw} h_0^2}{10^{-14}}\right) \tag{2}$$

for a scale-invariant stochastic gravitational-wave background. This represents a 500-fold improvement over the sensitivity of a single LISA interferometer. If it were not for the astrophysical foregrounds that are thought to dominate the CGB signal in the LISA band, a pair of LISA detectors would stand a good chance of detecting the CGB. In an effort to avoid being swamped by astrophysical sources, we focus our efforts on detecting the CGB below 1 μHz. We show that a pair of interferometers can reach a signal-to-noise ratio of

$$\mathrm{SNR} = 3.1 \left(\frac{T}{\mathrm{yr}}\right)^{1/2} \left(\frac{\Omega_{\mathrm{gw}} h_0^2}{10^{-14}}\right) \left(\frac{L}{\sqrt{3}\ \mathrm{AU}}\right)^2 \left(\frac{3 \times 10^{-16}\ \mathrm{m\ s^{-2}}}{\delta a}\right)^2 \left(\frac{f}{\mu\mathrm{Hz}}\right)^{3/2} \tag{3}$$

for a scale-invariant CGB spectrum. The above result is scaled against a possible LISA follow-on mission (LISA II) that calls for two identical interferometers, comprising six equally spaced spacecraft that form two equilateral triangles overlayed in a star pattern. The constellations follow circular orbits about the Sun in a common plane at a radius of 1 AU, so that each interferometer arm is $L = \sqrt{3}$ AU in length. The acceleration noise, δa, is scaled against a value that improves on the LISA specifications by one order of magnitude. The LISA II design could detect a stochastic background at 99% confidence with 1 yr of observations if $\Omega_{\mathrm{gw}} h_0^2 = 10^{-14}$. Ideally we would like to reach a sensitivity of at least $\Omega_{\mathrm{gw}} h_0^2 \sim 10^{-20}$ in order to detect inflationary spectra with a mild negative tilt. It is difficult to achieve this with spacecraft orbiting at 1 AU as thermal fluctuations due to solar heating of the spacecraft make it hard to reduce the acceleration noise below $\delta a \simeq 10^{-16}\,\mathrm{m\ s^{-2}}$. The best strategy is to increase the size of the orbit, R, as this increases the size of the interferometer, $L = \sqrt{3}R$, and decreases the thermal noise by R^{-2}.

2. Outline

We begin by deriving the response of a pair of cross-correlated space-based laser interferometers to a stochastic background of gravitational waves. Similar calculations have been done for ground-based detectors [14–18], but these omit the high-frequency transfer functions that play an important role in space-based systems. Our calculations closely follow those of Allen and Romano [18], and reduce to theirs in the low-frequency limit[2]. Many of the calculational details that we omit for brevity can be found in their paper. Having established the general formalism for cross-correlating space-based interferometers we use our results to identify some promising configurations for a gravitational background interferometer (GABI) mission to detect the CGB.

3. Detector response

We attack the problem of cross-correlating two space-based interferometers in stages. We begin by reviewing how the Doppler tracking of a pair of spacecraft can be used to detect gravitational waves. Using this result we derive the response of a two-arm Michelson interferometer and express the result in a convenient coordinate-invariant form. The response of a single interferometer is then used to find the sensitivity of a pair of cross-correlated space-based interferometers.

[2] Here high and low frequencies are defined relative to the *transfer frequency* of the detector $f_* = c/(2\pi L)$, where L is the length of one interferometer arm.

3.1. Single-arm Doppler tracking

Laser ranging can be used to monitor the proper distance between two spacecraft, thereby forming a gravitational wave detector [19]. A review of the Doppler tracking system can be found in appendix A. We find that the change, $\delta\ell$, in the optical path length, ℓ, caused by a gravitational wave propagating in the $\widehat{\Omega}$ direction with frequency f is given by

$$\frac{\delta\ell}{\ell} = \tfrac{1}{2}(\boldsymbol{u}\otimes\boldsymbol{u}) : \boldsymbol{h}(\widehat{\Omega}, f, \boldsymbol{x}, t)\, \mathcal{T}(\boldsymbol{u}\cdot\widehat{\Omega}, f). \tag{4}$$

Here $\boldsymbol{u}$ is a unit vector pointing from the first to the second spacecraft, $\boldsymbol{h}$ is the metric perturbation in the transverse-traceless gauge, the colon denotes the double contraction $\boldsymbol{a} : \boldsymbol{b} = a_{ij}b^{ij}$, and $\mathcal{T}$ is the transfer function

$$\begin{aligned}\mathcal{T}(\boldsymbol{u}\cdot\widehat{\Omega}, f) = \frac{1}{2}\Bigg[&\operatorname{sinc}\left(\frac{f}{2f_*}(1-\boldsymbol{u}\cdot\widehat{\Omega})\right)\exp\left(-\mathrm{i}\frac{f}{2f_*}(3+\boldsymbol{u}\cdot\widehat{\Omega})\right)\\ &+\operatorname{sinc}\left(\frac{f}{2f_*}(1+\boldsymbol{u}\cdot\widehat{\Omega})\right)\exp\left(-\mathrm{i}\frac{f}{2f_*}(1+\boldsymbol{u}\cdot\widehat{\Omega})\right)\Bigg],\end{aligned} \tag{5}$$

where $f_* = c/(2\pi L)$ is the *transfer frequency*. Waves with frequencies greater than f_* have wavelengths that are shorter than the mean distance between the spacecraft, L. The sinc function is defined such that $\operatorname{sinc}(x) = \sin(x)/x$.

3.2. Interferometer response

An interferometer can be formed by introducing a third spacecraft a distance L from the first spacecraft and differencing the outputs of the two arms[3]. The strain is given by

$$\begin{aligned}s(\widehat{\Omega}, f, \boldsymbol{x}, t) &= \frac{\delta\ell_{\boldsymbol{u}}(t) - \delta\ell_{\boldsymbol{v}}(t)}{\ell}\\ &= \boldsymbol{D}(\widehat{\Omega}, f) : \boldsymbol{h}(\widehat{\Omega}, f, \boldsymbol{x}, t),\end{aligned} \tag{6}$$

where

$$\boldsymbol{D}(\widehat{\Omega}, f) = \tfrac{1}{2}\left((\boldsymbol{u}\otimes\boldsymbol{u})\,\mathcal{T}(\boldsymbol{u}\cdot\widehat{\Omega}, f) - (\boldsymbol{v}\otimes\boldsymbol{v})\,\mathcal{T}(\boldsymbol{v}\cdot\widehat{\Omega}, f)\right) \tag{7}$$

is the detector response tensor and $\boldsymbol{u}$ and $\boldsymbol{v}$ are unit vectors in the direction of each interferometer arm, directed out from the vertex of the interferometer. The above expression gives the response of the interferometer to a plane wave of frequency f propagating in the $\widehat{\Omega}$ direction.

In appendix B the response of the interferometer to a stochastic background of gravitational waves is derived. The strength of the background is expressed in terms of the strain spectral density, $S_h(f)$, which is related to the energy density per logarithmic frequency interval by

$$\Omega_{\mathrm{gw}}(f) = \frac{4\pi^2}{3H_0^2} f^3 S_h(f). \tag{8}$$

The expectation value for the strain in the interferometer due to a stochastic gravitational-wave background is given by

$$\begin{aligned}\langle s(t)\rangle &= 0\\ \langle s^2(t)\rangle &= \int_0^\infty \mathrm{d}f\; S_h(f)\mathcal{R}(f),\end{aligned} \tag{9}$$

[3] More complicated differencing schemes have to be applied if the arms of the interferometer have unequal lengths in order to cancel laser phase noise [25].

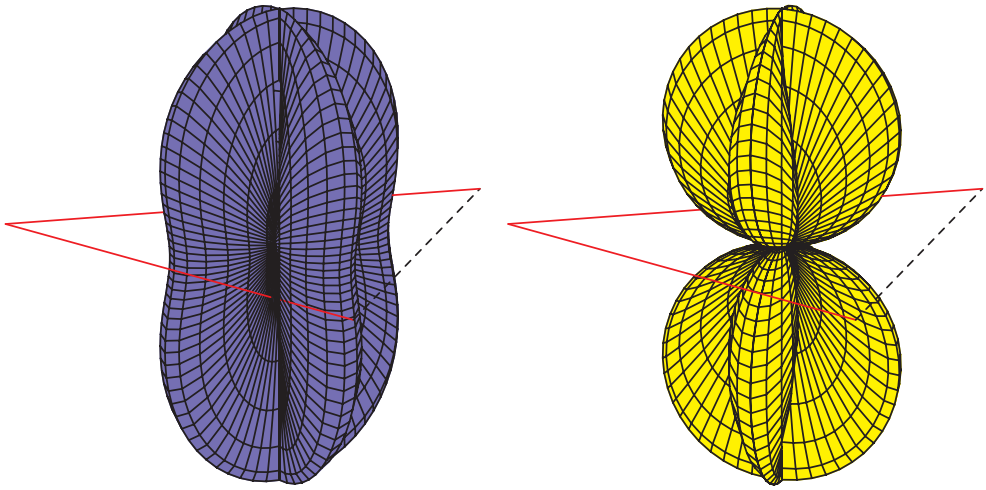

Figure 2. The magnitudes of the detector response functions $F^{+}(\hat{\Omega}, f)$ and $F^{\times}(\hat{\Omega}, f)$ in the low-frequency limit. The solid lines are the interferometer arms.

where $\mathcal{R}(f)$ is the transfer function

$$\mathcal{R}(f) = \int \frac{\mathrm{d}\hat{\Omega}}{4\pi} \sum_{A} F^{A}(\hat{\Omega}, f) F^{A}(\hat{\Omega}, f)^{*}, \tag{10}$$

and

$$F^{A}(\hat{\Omega}, f) = \boldsymbol{D}(\hat{\Omega}, f) : \boldsymbol{e}^{A}(\hat{\Omega}) \tag{11}$$

is the detector response function. The label $A = +, \times$ denotes the two polarizations of the gravitational wave and $\boldsymbol{e}^{+}$, $\boldsymbol{e}^{\times}$ are the polarization tensors.

The signal-to-noise ratio at frequency f is found to equal

$$\mathrm{SNR}(f) = \frac{S_h(f)\mathcal{R}(f)}{S_n(f)}, \tag{12}$$

where $S_n(f)$ is the spectral density of the noise in the interferometer. Sensitivity curves for space-based interferometers typically display the effective strain noise

$$\tilde{h}_{\mathrm{eff}}(f) \equiv \sqrt{\frac{S_n(f)}{\mathcal{R}(f)}}. \tag{13}$$

Signals with strain spectral densities $\tilde{h}(f)$ exceeding $\tilde{h}_{\mathrm{eff}}(f)$ can be detected with high confidence.

3.3. The LISA interferometer

As a concrete example of the general formalism described above, we derive the sensitivity curve for the LISA interferometer in appendix C.

The magnitudes of the LISA response functions $F^{+}(\hat{\Omega}, f)$ and $F^{\times}(\hat{\Omega}, f)$ are shown in figure 2 for $f \ll f_{*}$. They can be thought of as the polarization-dependent antenna patterns for the LISA detector responding to a stochastic background of gravitational waves[4].

[4] These shapes are not coordinate independent. They depend on how we choose $\boldsymbol{u}$ and $\boldsymbol{v}$ in relation to $\boldsymbol{e}^{+}$ and $\boldsymbol{e}^{\times}$.

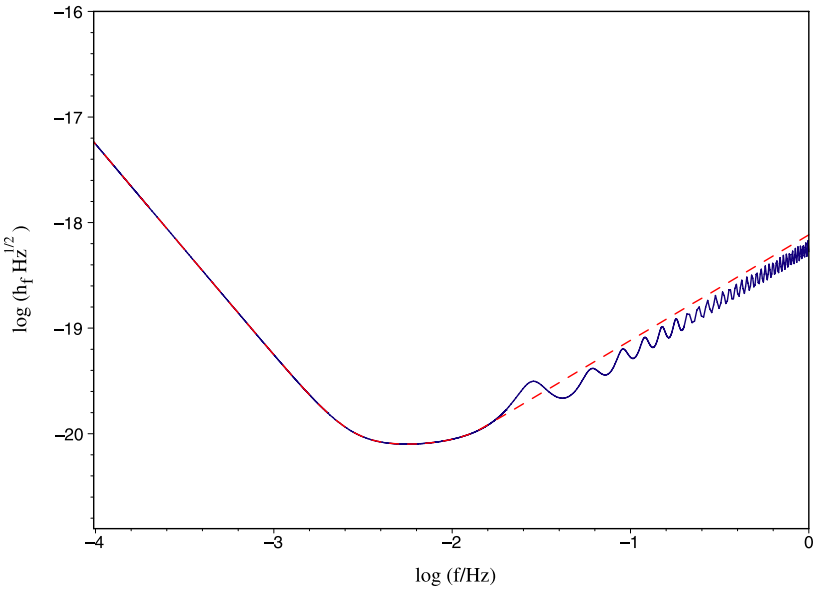

Figure 3. The effective noise floor for the LISA mission. The full curve was obtained numerically while the broken curve is our analytic approximation.

To estimate the effective strain spectral noise in the LISA detector, we need to calculate the transfer function $\mathcal{R}(f)$ and the noise spectral density $S_n(f)$. The noise spectral density can be estimated using values quoted in the LISA pre-phase A report [8]. The full transfer function has to be calculated numerically, but a good analytic approximation is given by

$$\mathcal{R}(f) = \begin{cases} \dfrac{3}{10}\left(1 - \dfrac{169}{504}\left(\dfrac{f}{f_*}\right)^2 + \dfrac{425}{9072}\left(\dfrac{f}{f_*}\right)^4 - \dfrac{165\,073}{47\,900\,160}\left(\dfrac{f}{f_*}\right)^6\right), & f < \frac{3}{2}f_* \\ \dfrac{16\,783\,143}{126\,156\,800}\left(\dfrac{3f_*}{2f}\right)^2, & f \geqslant \frac{3}{2}f_*. \end{cases} \tag{14}$$

The transfer frequency for LISA is $f_* = 9.54 \times 10^{-3}$ Hz. The sensitivity curve for the LISA detector is shown in figure 3.

4. Cross-correlating two interferometers

Having demonstrated that our formalism recovers the standard results for a single interferometer, we now investigate how the sensitivity can be improved by cross-correlating two interferometers. The most general expression for the cross-correlation of two detectors is given by

$$C = \int_{-T/2}^{T/2} \mathrm{d}t \int_{-T/2}^{T/2} \mathrm{d}t'\, S_1(t) S_2(t')\, Q(t - t'), \tag{15}$$

where $Q(t-t')$ is a filter function, T is the observation time and the S_i are the strain amplitudes read out from the ith detector.

In appendix D we calculate the response of the cross-correlated pair of detectors to a stochastic background of gravitational waves. The expectation value for C is given by

$$\langle C\rangle = \frac{T}{5}\sin^2\beta\int_{-\infty}^{\infty} \mathrm{d}f\, S_h(f)\gamma(f)\widetilde{Q}(f), \tag{16}$$

where β is the angle between the interferometer arms (we are assuming that the two interferometers have the same design), and $\gamma(f)$ is the overlap reduction function

$$\gamma(f) = \frac{5}{2\sin^2\beta}\int\frac{\mathrm{d}\widehat{\Omega}}{4\pi}\left(F_1^{+*}(\widehat{\Omega},f)F_2^{+}(\widehat{\Omega},f) + F_1^{\times *}(\widehat{\Omega},f)F_2^{\times}(\widehat{\Omega},f)\right)\mathrm{e}^{-2\pi\mathrm{i}f\widehat{\Omega}\cdot(\boldsymbol{x}_1-\boldsymbol{x}_2)/c}. \tag{17}$$

Here $\boldsymbol{x}_i$ denotes the position of the corner spacecraft in each interferometer. The term 'overlap reduction function' refers to the fact that $\gamma(f)$ takes into account the misalignment and separation of the interferometers. In addition, $\gamma(f)$ contains the transfer functions for each detector, as can be seen by setting $F_1 = F_2$ in (17) and comparing with (10):

$$\gamma_{1=2}(f) = \frac{5}{2\sin^2\beta}\mathcal{R}(f). \tag{18}$$

The key idea behind cross-correlating two detectors is that the noise in each detector is uncorrelated, while the response to the gravitational-wave background is correlated. That is why the expression for $\langle C\rangle$ involves the signal strength, S_h, but not the noise in each detector, S_{n1} or S_{n2}. In appendix D we show that the signal-to-noise ratio for the cross-correlated signal,

$$\mathrm{SNR} = \frac{\langle C\rangle}{\sqrt{\langle C^2\rangle - \langle C\rangle^2}}, \tag{19}$$

is maximized by the optimal filter

$$\widetilde{Q}(f) = \frac{S_h(f)\gamma^*(f)}{M(f)}, \tag{20}$$

where

$$\begin{aligned} M(f) = {} & S_{n1}(f)\,S_{n2}(f) + S_{n1}(f)S_h(f)\mathcal{R}_2(f) + S_{n2}(f)S_h(f)\mathcal{R}_1(f) \\ & + S_h^2(f)\left(\tfrac{4}{25}\sin^4\beta\,|\gamma(f)|^2 + \mathcal{R}_1(f)\mathcal{R}_2(f)\right). \end{aligned} \tag{21}$$

Using this filter, the optimal signal-to-noise ratio for the cross correlated interferometers is given by

$$\mathrm{SNR}^2 = \frac{8T}{25}\sin^4\beta\int_0^{\infty}\mathrm{d}f\,\frac{|\gamma(f)|^2 S_h^2(f)}{M(f)}. \tag{22}$$

In the limit that the noise power in each interferometer is very much larger than the signal power we find

$$\mathrm{SNR}^2 = \frac{9H_0^4\sin^4\beta}{50\pi^4}\,T\int_0^{\infty}\mathrm{d}f\,\frac{|\gamma(f)|^2\,\Omega_{\mathrm{gw}}^2(f)}{f^6 S_{n1}(f)S_{n2}(f)}, \tag{23}$$

which recovers the expressions quoted by Flanagan [16] and Allen [17] when we set $\beta = \pi/2$. The factor of $\sin^4\beta$ was missed in these papers, as the implicit assumption that $\beta = \pi/2$ crept into supposedly general expressions. The main new ingredient in our expression are the transfer functions $\mathcal{T}_i(f)$ that reside in the overlap reduction function $\gamma(f)$. The transfer functions prevent us from performing the integral over the 2-sphere in equation (17) in closed

form except in the high- or low-frequency limits. However, it is a simple matter to evaluate $\gamma(f)$ numerically for a given detector configuration. In the next section we evaluate the overlap reduction function for a pair of LISA interferometers. A similar calculation has been performed by Ungarelli and Vecchio [20] using the formalism developed by Allen and Romano [18] for ground-based detectors. Unfortunately, the overlap reduction functions calculated by Ungarelli and Vecchio are missing the transfer functions which play a crucial role in space-based systems such as LISA.

If we are trying to detect a weak stochastic background with a noisy detector, then equation (23) is the appropriate expression to use for the signal-to-noise ratio. However, there may be some range of frequencies where the signal power dominates the noise power in each detector. The contribution to the SNR from a clean frequency window of this sort is given by

$$\mathrm{SNR}^2(f, \Delta f) = 2T \int_{f-\Delta f/2}^{f+\Delta f/2} \mathrm{d}f' \, \frac{|\gamma(f')|^2}{\left(|\gamma(f')|^2 + \mathcal{R}_1(f')\mathcal{R}_2(f')/(\frac{2}{5}\sin^2\beta)^2\right)}. \tag{24}$$

The integrand is approximately equal to $\frac{1}{2}$ for all frequencies, so that

$$\mathrm{SNR}(f, \Delta f) \simeq \sqrt{T\,\Delta f}. \tag{25}$$

This expression provides a useful lower bound for the SNR that can be achieved for detectors with a clean frequency window of width Δf centred at some frequency f. For example, the spectral density due to white dwarf binaries in our galaxy is expected to exceed LISA's noise spectral density for frequencies in the range $10^{-4} \rightarrow 3 \times 10^{-3}$ Hz. To detect this background at 90% confidence requires a signal-to-noise ratio of 1.65, which can be achieved with just 15 min of integration time.

4.1. Cross-correlating two LISA interferometers

One possible modification to the current LISA proposal [8] would be to fly six spacecraft instead of three, to form two independent interferometers. The cost of flying six spacecraft is far less than twice the cost of flying three spacecraft, and has the advantage of providing additional redundancy to the mission. How would we best use a pair of LISA interferometers? If our main concern is getting better positional information on bright astrophysical sources, then we would fly the two interferometers far apart, e.g. with one leading and the other trailing the Earth. However, if we want to maximize the cross-correlation then we need the interferometers to be coincident and coaligned. However, a configuration of this type is likely to share correlated noise sources, which would defeat the purpose of cross-correlating the interferometers. A better choice is to use a configuration that is coaligned but not coincident. This can be done by placing six spacecraft at the corners of a regular hexagon as shown in figure 5. Note that interferometers have parallel arms and that the corner spacecraft are separated by the diameter of the circle. The hexagonal configuration will suffer correlated buffeting from variations in the solar flux, but this will not necessarily translate into correlated noise in the two interferometers as the response of the drag-free systems in each spacecraft, which is the cause of the acceleration noise discussed in appendix B, will be uncorrelated.

Using the same coordinate system that we used for a single interferometer in appendix C, the unit vectors $\boldsymbol{u}_i$ and $\boldsymbol{v}_i$ along each interferometer arm are

$$\begin{aligned} \boldsymbol{u}_1 &= -\boldsymbol{u}_2 = \frac{1}{2}\hat{x} + \frac{\sqrt{3}}{2}\hat{y} \\ \boldsymbol{v}_1 &= -\boldsymbol{v}_2 = -\frac{1}{2}\hat{x} + \frac{\sqrt{3}}{2}\hat{y}, \end{aligned} \tag{26}$$

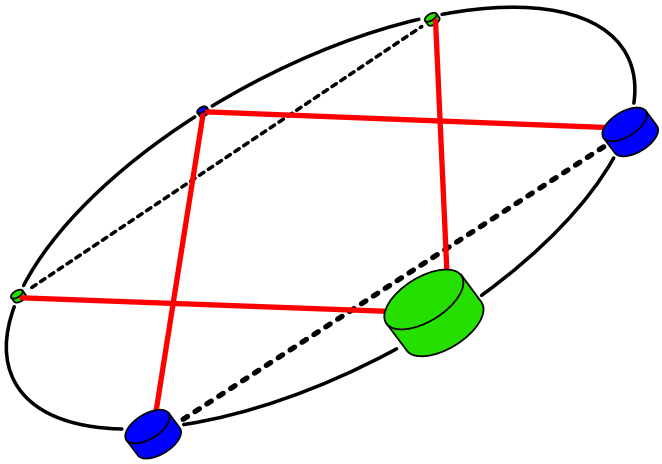

Figure 4. The hexagonal cross-correlation pattern.

where the index $i = 1, 2$ labels the two interferometers. The displacement of the corner spacecraft is given by

$$\boldsymbol{x}_1 - \boldsymbol{x}_2 = -2R\,\hat{y} \tag{27}$$

where R is the radius of the circle. The angle between the interferometer arms is $\beta = \pi/3$, and the length of each arm is $L = \sqrt{3}R$. The light crossing time between the two interferometers, $2R/c$, is almost equal to the light crossing time along each interferometer arm, $\sqrt{3}R/c$. Thus, the loss of sensitivity due to multiple wavelengths fitting between the interferometers occurs for frequencies near the transfer frequency f_* (the transfer frequency corresponds to wavelengths that fit inside the interferometer arms).

The various ingredients we need to calculate $\gamma(f)$ follow from those given in equations (C3)–(C8). Putting everything together in (D8) and working in the low-frequency limit we find

$$\gamma(f) = 1 - \frac{383}{504}\left(\frac{f}{f_*}\right)^2 + \frac{893}{3888}\left(\frac{f}{f_*}\right)^4 - \frac{5414\,989}{143\,700\,480}\left(\frac{f}{f_*}\right)^6 + \cdots. \tag{28}$$

For frequencies above f_* the overlap reduction function decays as f^{-3}. A numerically generated plot of $\gamma(f)$ is displayed in figure 5. Scaling the signal-to-noise ratio (23) in units appropriate to a pair of LISA interferometers we have

$$\mathrm{SNR}^2 = 34.4\left(\frac{T}{\mathrm{yr}}\right)\int_0^\infty \left(\frac{\mathrm{d}f}{\mathrm{mHz}}\right)|\gamma(f)|^2\left(\frac{\Omega_{\mathrm{gw}}(f)h_0^2}{10^{-15}}\right)^2\left(\frac{\mathrm{mHz}}{f}\right)^6\left(\frac{10^{-41}\ \mathrm{Hz}^{-1}}{S_n(f)}\right)^2. \tag{29}$$

Using equation (C15) for $S_n(f)$ and assuming a scale-invariant stochastic background yields a signal-to-noise ratio of

$$\mathrm{SNR} = 1.44\sqrt{\frac{T}{\mathrm{yr}}}\left(\frac{\Omega_{\mathrm{gw}}h_0^2}{10^{-14}}\right). \tag{30}$$

This represents a 500-fold improvement on the sensitivity of a single LISA detector. Indeed, if it were not for the astrophysical foregrounds, a pair of LISA detectors would be well poised to detect a scale-invariant gravitational-wave background from inflation.

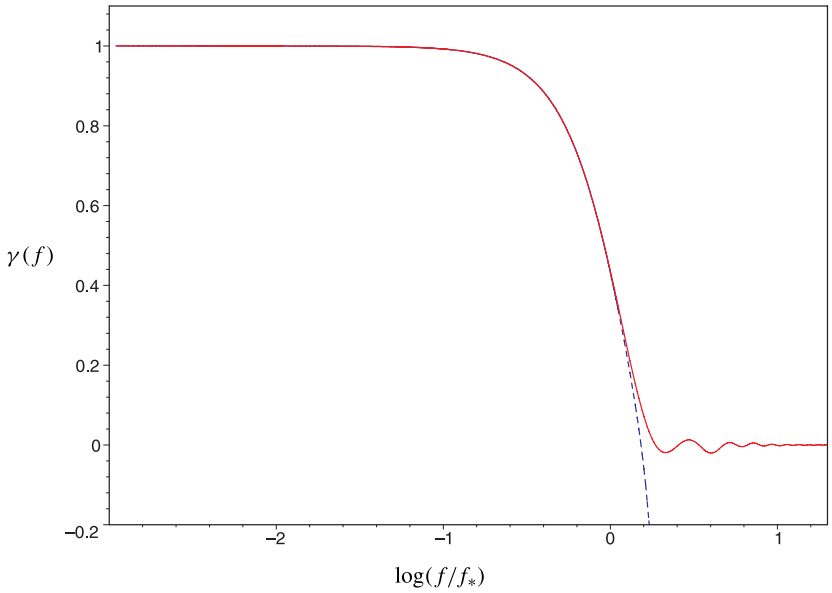

Figure 5. The overlap reduction function for the hexagonal cross-correlation pattern. The full curve was generated numerically while the broken curve is our analytic approximation from equation (28).

5. Missions to detect the CGB

We will work on the assumption that astrophysical foregrounds swamp the CGB for frequencies above a few μHz, and design our missions accordingly. What we have in mind is a post-LISA mission based on the (by then) tried and tested LISA technology, but with some allowance for improvements in basic technologies such as the accelerometers. Since cross-correlating two interferometers at ultra-low frequencies does not buy us a major improvement in sensitivity, we need to start with a design that has excellent sensitivity at low frequencies. Basically this means building bigger interferometers with better accelerometers. To be concrete, we show the sensitivity curves for three generations of LISA missions in figure 6. LISA I corresponds to the current LISA design with the spacecraft cartwheeling about the Sun at 1 AU, separated by $L = 5 \times 10^9$ m. LISA II refers to a possible follow on mission with the three spacecraft evenly spaced around an orbit at 1 AU, so that the spacecraft are separated by $L = \sqrt{3}$ AU. The LISA II mission would use similar optics[5] to LISA I (same laser power and telescope size), but allows for an order of magnitude improvement in accelerometer performance. LISA III is similar to LISA II, except that the constellation would orbit at 35 AU (between Neptune and Pluto) and the accelerometers would be improved by a further two orders of magnitude. The acceleration noise for LISA III would benefit from the three orders of magnitude reduction in solar radiation relative to LISAs I and II, but this would come at the cost of having to power the spacecraft using nuclear generators (RTGs).

[5] The main difference is that we have to 'lead our target' by a much larger amount for the LISA II mission. In other words, the angle, $\Delta\theta$, between the received and transmitted laser beams is much larger for LISA II than for LISA I. A simple calculation yields $\Delta\theta = 2v/c$, where v is the velocity around the circle shown in figure 4. For LISA II $v/c = (GM_\odot/c^2/R)^{1/2}$, while for LISA I $v/c = 2e(GM_\odot/c^2/R)^{1/2}$. Here $e = 0.01$ is the eccentricity of the LISA I orbits and $R = 1$ AU. This equates to lead of $\Delta\theta = 4 \times 10^{-6}$ radians for LISA I and $\Delta\theta = 2 \times 10^{-4}$ rad for LISA II.

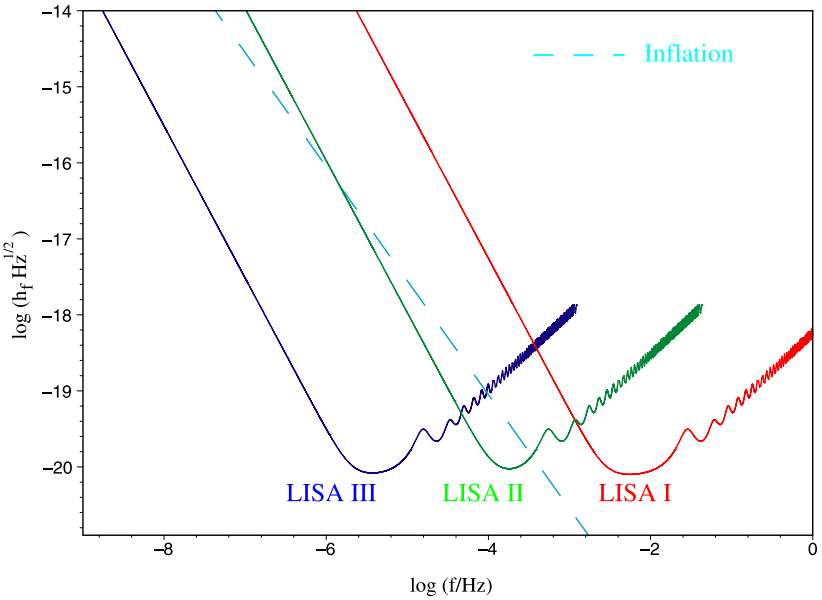

Figure 6. Sensitivity curves for three generations of LISA missions. Also shown is a prediction for the CGB in a scale-invariant inflationary scenario.

For all three missions we see that the μHz range lies well below the interferometer's transfer frequency

$$f_* = 1.84 \times 10^{-4} \left(\frac{\sqrt{3}\ \mathrm{AU}}{L} \right) \ \mathrm{Hz}. \tag{31}$$

Indeed, it would take a mission orbiting at 180 AU (somewhere inside the Kuiper belt) to achieve a transfer frequency of $f_* = 10^{-6}$ Hz. In practical terms this allows us to work in the low-frequency limit $f \ll f_*$ where it is easy to derive analytic expressions for the overlap reduction function $\gamma(f)$. Moreover, we need only consider acceleration noise when working below 1 μHz. All our calculations are based on the same hexagonal cross-correlation shown in figure 4 that we used for the LISA I cross-correlation. Using equation (C14) for the acceleration noise and ignoring the position noise yields

$$S_n(f) = 3.42 \times 10^{-33} \left(\frac{\sqrt{3}\ \mathrm{AU}}{L} \right)^2 \left(\frac{\mu\mathrm{Hz}}{f} \right)^4 \left(\frac{\delta a}{3 \times 10^{-16}\ \mathrm{m\ s^{-2}}} \right)^2 \mathrm{Hz}^{-1}. \tag{32}$$

In the limit that the noise power dominates the spectral density of the CGB we arrive at an estimate for the signal-to-noise ratio for frequencies below 1 μHz

$$\mathrm{SNR}^2 = 29.4 \left(\frac{T}{\mathrm{yr}} \right) \left(\frac{L}{\sqrt{3}\ \mathrm{AU}} \right)^4 \left(\frac{3 \times 10^{-16}\ \mathrm{m\ s^{-2}}}{\delta a} \right)^4 \times \int_0^f |\gamma(f')|^2 \left(\frac{\Omega_{\mathrm{gw}}(f') h_0^2}{10^{-14}} \right)^2 \left(\frac{f'}{\mu\mathrm{Hz}} \right)^2 \left(\frac{\mathrm{d}f'}{\mu\mathrm{Hz}} \right). \tag{33}$$

The SNR is scaled against the LISA II specifications. Since $f/f_* \ll 1$ it is a good approximation to set $\gamma(f) = 1$ inside the integral. We model the CGB spectrum near 1 μHz by a simple power law:

$$\Omega_{\rm gw}(f) = \Omega_{\mu\rm Hz}\left(\frac{f}{\mu\rm Hz}\right)^{\alpha}, \tag{34}$$

scaled relative to a reference value at 1 μHz. With these approximations we arrive at our final expression for the SNR for a pair of cross-correlated interferometers in the ultra-low-frequency regime:

$$\rm SNR = \frac{3.13}{\sqrt{1+2\alpha/3}}\left(\frac{T}{\rm yr}\right)^{1/2}\left(\frac{L}{\sqrt{3}\ \rm AU}\right)^{2}\left(\frac{3\times10^{-16}\ \rm m\ s^{-2}}{\delta a}\right)^{2}\left(\frac{\Omega_{\mu\rm Hz}\,h_0^2}{10^{-14}}\right)\left(\frac{f}{\mu\rm Hz}\right)^{\alpha+3/2}. \tag{35}$$

We can compare this with the SNR of a single interferometer in the ultra-low-frequency regime by combining equations (B8), (B18) and (32) to find

$$\rm SNR_{\it s}(\it f) = 0.683\left(\frac{L}{\sqrt{3}\ \rm AU}\right)^{2}\left(\frac{3\times10^{-16}\ \rm m\ s^{-2}}{\delta a}\right)^{2}\left(\frac{\Omega_{\mu\rm Hz}\,h_0^2}{10^{-14}}\right)\left(\frac{f}{\mu\rm Hz}\right)^{\alpha+1}. \tag{36}$$

We see that the individual and cross-correlated sensitivities are related

$$\rm SNR = \frac{0.82}{\sqrt{1+2\alpha/3}}\,(\it T\Delta f)^{1/2}\,\rm SNR_{\it s}(\it f), \qquad \rm for \quad \it f \approx \Delta f \approx 1\ \mu\rm Hz. \tag{37}$$

This supports our earlier assertion that cross-correlating two interferometers improves on the sensitivity of a single interferometer by $(T\Delta f)^{1/2}$, where Δf is approximately equal to the central observing frequency f.

Equation (35) tells us that a gravitational background interferometer built from two LISA II interferometers could detect the CGB at greater than 90% confidence with 1 yr of data taking if $\Omega_{\rm gw}(1\ \mu\rm Hz)h_0^2 = 10^{-14}$. The same equation also tells us what has to be done to achieve greater sensitivity. It is clear that increasing the duration of the mission is not the best answer as the SNR only improves as the square root of the observation time. In contrast, increasing the size of the interferometer or reducing the acceleration noise produces a quadratic increase in sensitivity. For example, a GABI detector built from a pair of LISA III interferometers could detect the CGB at 90% confidence for signals as small as $\Omega_{\rm gw}(1\ \mu\rm Hz)h_0^2 = 4\times10^{-22}$. In fact, for signal strengths above this value the LISA III detectors are signal dominated and we need to use equation (25) instead of (35) to calculate the SNR.

We can also use equation (35) to determine how well a GABI mission can measure the CGB power spectrum. Suppose that we break up the frequency spectrum into bins of width δf. Nyquist's theorem tells us that $\delta f \geqslant 1/T$, e.g. for an observation time of 1 yr the frequency resolution is 3.17×10^{-8} Hz. Writing $\delta f = n/T$ where $n \geqslant 1$, and taking $\delta f \ll f$, we find from (35) that in the frequency window $(f - \delta f/2,\ f + \delta f/2)$ the SNR is

$$\rm SNR(\it f, \delta f) = 0.965\sqrt{\it n}\left(\frac{L}{\sqrt{3}\ \rm AU}\right)^{2}\left(\frac{3\times10^{-16}\ \rm m\ s^{-2}}{\delta a}\right)^{2}\left(\frac{\Omega_{\mu\rm Hz}\,h_0^2}{10^{-14}}\right)\left(\frac{f}{\mu\rm Hz}\right)^{\alpha+1}. \tag{38}$$

We see that the SNR in each frequency bin scales as $f^{1+\alpha}$. For a scale-invariant spectrum ($\alpha = 0$) this translates into poor performance at frequencies below 1 μHz and limits the range over which we can measure the spectrum. For example, if the CGB has a scale-invariant spectrum and an amplitude of $\Omega_{\rm gw}h_0^2 \geqslant 2\times10^{-13}$, a pair of LISA II interferometers could measure the spectrum over the range $10^{-7} \rightarrow 10^{-6}$ Hz. For a pair of LISA III detectors the

main limitation at low frequencies comes from Nyquist's theorem. Since mission lifetimes are limited to tens of years, it will not be possible to measure the CGB spectrum much below 10^{-8} Hz using space-based interferometers. Indeed, it may be difficult to push much below 10^{-7} Hz unless ways can be found to build detectors that are stable for many months. A pair of LISA III interferometers could measure the spectrum between $10^{-8} \rightarrow 10^{-6}$ Hz if $\Omega_{\rm gw}(10^{-8}\ {\rm Hz})h_0^2 \geqslant 10^{-18}$. To measure the CGB spectrum below 10^{-8} Hz requires a return, full circle, to the world of CMB physics. Detailed polarization measurements of the CMB can be used to infer [21] the CGB power spectrum for frequencies in the range $10^{-18} \rightarrow 10^{-16}$ Hz.

6. Discussion

The LISA follow-on missions we have described will be able to detect or place stringent bounds on the CGB amplitude and spectrum between 10^{-8} and 10^{-6} Hz. However, how can we be sure that it is the CGB we have detected and not some unresolved astrophysical foreground? The answer can be found in the statistical character of the competing signals. Most early-universe theories predict that the CGB is truly stochastic. In contrast, the astrophysical signal is only approximately stochastic, in a sense that can be made precise by appealing to the central limit theorem.

The extragalactic x-ray background (XRB) provides a good analogy for the astrophysical gravitational-wave background. Measurements made by the COBE satellite imply that less than 3% of the XRB comes from diffuse hot gas [4], so a large collection of discrete sources must be responsible. Surveys by the Röntgen Satellite (ROSAT) at a flux limit of 2×10^{-14} erg cm^{-2} s^{-1} found that over 30% of XRB in the energy range 0.5–2.0 keV could be accounted for by individual quasi-stellar objects [22]. Later ROSAT surveys at the improved flux limit of 1.6×10^{-15} erg cm^{-2} s^{-1} were able to resolve most of the remaining contributions to the XRB [23]. They found that 84% of the XRB could be accounted for by individual quasi-stellar objects, with the remainder coming from narrow emission line galaxies and galaxy clusters at redshifts $z > 0.3$. The lesson is that what appears as a stochastic background to an instrument with poor resolution and sensitivity is in fact a confusion-limited signal that can have its true character exposed by measurements with greater sensitivity and improved angular and/or frequency resolution.

The curve in figure 1 labelled 'astrophysical foregrounds' is the estimated confusion limit caused by various extra-galactic astrophysical sources of gravitational waves. It marks the amplitude at which we can expect to find, on average, one source per frequency bin[6]. For signal strengths smaller than the confusion limit there will be multiple sources in each frequency bin. However, the astrophysical signal only starts to look truly stochastic for amplitudes far below the confusion limit, as it takes thousands of sources contributing to each frequency bin to simulate a stochastic signal. Even then, the astrophysical foregrounds will have tell-tale bright outliers whose number and distribution can be predicted on statistical grounds. If we do not see these outliers, then we can safely conclude that we have detected the CGB.

Acknowledgments

We thank Peter Bender and Raffaella Schneider for sharing their thoughts on possible astrophysical sources of gravitational waves.

[6] The confusion limit goes down when the frequency resolution goes up. Most plots of the confusion limit assume a one year observation period so the bins are 3.17×10^{-8} Hz in width.

Appendix A. Doppler tracking

Following the treatment of Hellings [19], we consider two free spacecraft, one at the origin of a coordinate system and the other a distance L away at an angle θ from the z-axis. Both spacecraft are at rest in this coordinate system. The spacecraft at the origin sends out a series of photons, while a weak plane gravitational wave is passing through space in the $+z$ direction. To leading order, the spacetime metric in the transverse-traceless gauge is

$$\mathrm{d}s^2 = -c^2\,\mathrm{d}t^2 + \mathrm{d}z^2 + (1 + h\cos 2\psi)\,\mathrm{d}x^2 + (1 - h\cos 2\psi)\,\mathrm{d}y^2 - h\sin 2\psi\,\mathrm{d}x\,\mathrm{d}y, \tag{A1}$$

where $h(t - z/c)$ is the wave amplitude and ψ is the angle between the principal polarization vector and the x-axis. Choosing our coordinates such that the second spacecraft is in the x–z plane, the path of the photons can be parametrized by

$$x = \rho\sin\theta \qquad z = \rho\cos\theta. \tag{A2}$$

The photon path in the perturbed spacetime is given by $\mathrm{d}s^2 = 0$, or

$$c\,\mathrm{d}t \simeq \pm\big(1 + \tfrac{1}{2}h\cos 2\psi\,\sin^2\theta\big)\,\mathrm{d}\rho. \tag{A3}$$

The round-trip journey from spacecraft 1 to spacecraft 2 and back again is given by

$$\ell(t_2 - t_0) = \int_{t_0}^{t_2} c\,\mathrm{d}t = 2L + \tfrac{1}{2}\cos 2\psi\,\sin^2\theta\left(\int_0^L h\left[t_0 + \frac{\rho}{c}(1 - \cos\theta)\right]\mathrm{d}\rho + \int_0^L h\left[t_1 + \frac{L}{c} - \frac{\rho}{c}(1 + \cos\theta)\right]\mathrm{d}\rho\right). \tag{A4}$$

Here t_0 is the time of emission, t_1 is the time of reception at spacecraft 2 and t_2 is the time of reception back at the first spacecraft. Using $h(q) = h_0\exp(\mathrm{i}\omega q)$, the varying portion of the round-trip distance is

$$\delta\ell(t_2) = L\,h(t_2)\cos 2\psi\,\sin^2\theta\,\frac{1}{2}\left(\operatorname{sinc}\left(\frac{f}{2f_*}(1 - \cos\theta)\right)\exp\left(-\mathrm{i}\frac{f}{2f_*}(3 + \cos\theta)\right) + \operatorname{sinc}\left(\frac{f}{2f_*}(1 + \cos\theta)\right)\exp\left(-\mathrm{i}\frac{f}{2f_*}(1 + \cos\theta)\right)\right), \tag{A5}$$

where $f = \omega/(2\pi)$ is the frequency of the gravitational wave and $f_* = c/(2\pi L)$ is the transfer frequency. To zeroth order in h, the optical path length is $\ell = 2L$. The general, coordinate-independent version of this expression is given by

$$\frac{\delta\ell}{\ell} = \tfrac{1}{2}(\boldsymbol{u}\otimes\boldsymbol{u}) : \boldsymbol{h}(\widehat{\Omega})\,\mathcal{T}(\boldsymbol{u}\cdot\widehat{\Omega}, f), \tag{A6}$$

where $\boldsymbol{u}$ is a unit vector pointing from the first to the second spacecraft and $\widehat{\Omega}$ is a unit vector in the direction the gravitational wave is propagating. The colon denotes the double contraction $\boldsymbol{a} : \boldsymbol{b} = a_{ij}b^{ij}$. The transfer function $\mathcal{T}$ is given by

$$\mathcal{T}(\boldsymbol{u}\cdot\widehat{\Omega}, f) = \tfrac{1}{2}\left[\operatorname{sinc}\left(\frac{f}{2f_*}(1 - \boldsymbol{u}\cdot\widehat{\Omega})\right)\exp\left(-\mathrm{i}\frac{f}{2f_*}(3 + \boldsymbol{u}\cdot\widehat{\Omega})\right) + \operatorname{sinc}\left(\frac{f}{2f_*}(1 + \boldsymbol{u}\cdot\widehat{\Omega})\right)\exp\left(-\mathrm{i}\frac{f}{2f_*}(1 + \boldsymbol{u}\cdot\widehat{\Omega})\right)\right]. \tag{A7}$$

This expression for $\mathcal{T}$ agrees with that derived by Schilling [24]. The gravitational wave is described by the tensor

$$\boldsymbol{h}(t, \boldsymbol{x}) = h^+(\omega t - \omega\widehat{\Omega}\cdot\boldsymbol{x})\boldsymbol{\epsilon}^+(\widehat{\Omega}, \psi) + h^\times(\omega t - \omega\widehat{\Omega}\cdot\boldsymbol{x})\boldsymbol{\epsilon}^\times(\widehat{\Omega}, \psi), \tag{A8}$$

with polarization tensors

$$\begin{aligned}\boldsymbol{\epsilon}^{+}(\widehat{\Omega},\psi) &= \boldsymbol{e}^{+}(\widehat{\Omega})\cos 2\psi - \boldsymbol{e}^{\times}(\widehat{\Omega})\sin 2\psi \\ \boldsymbol{\epsilon}^{\times}(\widehat{\Omega},\psi) &= \boldsymbol{e}^{+}(\widehat{\Omega})\sin 2\psi + \boldsymbol{e}^{\times}(\widehat{\Omega})\cos 2\psi.\end{aligned} \tag{A9}$$

The basis tensors can be written as

$$\begin{aligned}\boldsymbol{e}^{+}(\widehat{\Omega}) &= \hat{m}\otimes\hat{m} - \hat{n}\otimes\hat{n} \\ \boldsymbol{e}^{\times}(\widehat{\Omega}) &= \hat{m}\otimes\hat{n} + \hat{n}\otimes\hat{m}\end{aligned} \tag{A10}$$

where $\hat{m}$, $\hat{n}$ and $\widehat{\Omega}$ are an orthonormal set of unit vectors. The expression in (A5) can be recovered from (A6) by setting

$$\begin{aligned}&h^{+} = h, \qquad h^{\times} = 0, \qquad \widehat{\Omega} = \hat{z}, \qquad \boldsymbol{u} = \hat{x}\sin\theta + \hat{z}\cos\theta, \\ &\boldsymbol{e}^{+} = \hat{x}\otimes\hat{x} - \hat{y}\otimes\hat{y}, \qquad \text{and} \qquad \boldsymbol{e}^{\times} = \hat{x}\otimes\hat{y} + \hat{y}\otimes\hat{x}.\end{aligned} \tag{A11}$$

The transfer function $\mathcal{T}$ approaches unity for $f \ll f_*$, and falls of as $1/f$ for $f \gg f_*$ by virtue of the sinc function. For a ground-based detector such as LIGO the transfer function can be ignored since instrument noise keeps the operational range below LIGO's transfer frequency of $f_* \approx 10^4$ Hz (not to mention that LIGO is a Fabry–Perot interferometer so our results do not really apply [15]). For a space-based detector such as LISA, the instrument noise does not rise appreciably at high frequencies, and it is the transfer function that limits the high-frequency response. The sinc function is responsible for the wiggly rise in the LISA sensitivity curve at high frequency that can be seen in figure 3.

Appendix B. Interferometer response to a stochastic background

A general gravitational-wave background can be expanded in the terms of plane waves:

$$\begin{aligned}h_{ij}(t,\boldsymbol{x}) &= \int_{-\infty}^{\infty} \mathrm{d}f \int \mathrm{d}\widehat{\Omega}\, \tilde{h}_{ij}(\widehat{\Omega}, f, \boldsymbol{x}, t) \\ &= \sum_{A}\int_{-\infty}^{\infty} \mathrm{d}f \int \mathrm{d}\widehat{\Omega}\, \tilde{h}_{A}(f,\widehat{\Omega})\mathrm{e}^{-2\pi \mathrm{i} f t}\mathrm{e}^{2\pi \mathrm{i} f \widehat{\Omega}\cdot\boldsymbol{x}/c} e^{A}_{ij}(\widehat{\Omega}).\end{aligned} \tag{B1}$$

Here $\int \mathrm{d}\widehat{\Omega} = \int_0^{2\pi}\mathrm{d}\phi\int_0^{\pi}\sin\theta\,\mathrm{d}\theta$ denotes an all-sky integral. The Fourier amplitudes obey $\tilde{h}_A(-f) = \tilde{h}^{*}_{A}(f)$ since the waves have real amplitudes. In the final expression we have chosen $\boldsymbol{e}^{+}$ and $\boldsymbol{e}^{\times}$ as basis tensors for the decomposition of the two independent polarizations. The response of the detector (which we are free to locate at $\boldsymbol{x} = \boldsymbol{0}$) to a superposition of plane waves is then

$$\begin{aligned}s(t) &= \int_{-\infty}^{\infty} \mathrm{d}f \int \mathrm{d}\widehat{\Omega}\, s(\widehat{\Omega}, f, \boldsymbol{0}, t) \\ &= \sum_{A}\int_{-\infty}^{\infty} \mathrm{d}f \int \mathrm{d}\widehat{\Omega}\, \tilde{h}_{A}(f,\widehat{\Omega})\mathrm{e}^{-2\pi \mathrm{i} f t}\, \boldsymbol{D}(\widehat{\Omega}, f) : \boldsymbol{e}^{A}(\widehat{\Omega}).\end{aligned} \tag{B2}$$

From this we infer that the Fourier transform of $s(t)$ is given by

$$\tilde{s}(f) = \sum_{A}\int \mathrm{d}\widehat{\Omega}\, \tilde{h}_{A}(f,\widehat{\Omega})\boldsymbol{D}(\widehat{\Omega}, f) : \boldsymbol{e}^{A}(\widehat{\Omega}). \tag{B3}$$

In the low-frequency limit the transfer function $\mathcal{T}$ approaches unity and $\boldsymbol{D}(\widehat{\Omega}, f)$ only depends on the geometry of the detector:

$$\boldsymbol{D} = \tfrac{1}{2}\,(\boldsymbol{u}\otimes\boldsymbol{u} - \boldsymbol{v}\otimes\boldsymbol{v}). \tag{B4}$$

To a first approximation, a stochastic gravitational-wave background can be taken to be isotropic, stationary and unpolarized. It is fully specified by the ensemble averages:

$$\langle \tilde{h}_A(f,\widehat{\Omega})\rangle = 0, \qquad \langle \tilde{h}_A(f,\widehat{\Omega})\tilde{h}_{A'}(f',\widehat{\Omega}')\rangle = 0, \tag{B5}$$

and

$$\langle \tilde{h}^*_A(f,\widehat{\Omega})\tilde{h}_{A'}(f',\widehat{\Omega}')\rangle = \tfrac{1}{2}\delta(f-f')\frac{\delta^2(\widehat{\Omega},\widehat{\Omega}')}{4\pi}\delta_{AA'}\,S_h(f). \tag{B6}$$

Here $S_h(f)$ is the spectral density of the stochastic background and the normalization is chosen such that

$$\begin{aligned}\langle \tilde{h}^*_A(f)\tilde{h}_{A'}(f')\rangle &\equiv \int \mathrm{d}\widehat{\Omega}\,\mathrm{d}\widehat{\Omega}'\,\langle \tilde{h}^*_A(f,\widehat{\Omega})\,\tilde{h}_{A'}(f',\widehat{\Omega}')\rangle \\ &= \tfrac{1}{2}\delta(f-f')\delta_{AA'}\,S_h(f).\end{aligned} \tag{B7}$$

The spectral density has dimension Hz^{-1} and satisfies $S_h(f) = S_h(-f)$. It is related to $\Omega_{\mathrm{gw}}(f)$ by

$$\Omega_{\mathrm{gw}}(f) = \frac{4\pi^2}{3H_0^2}f^3 S_h(f). \tag{B8}$$

The time-averaged response[7] of the interferometer,

$$\langle s(t)\rangle_\tau = \lim_{\tau\to\infty}\frac{1}{\tau}\int_{-\tau/2}^{\tau/2} s(t)\,\mathrm{d}t, \tag{B9}$$

when applied to a stochastic background, is equivalent to the ensemble average

$$\begin{aligned}\langle s(t)\rangle_\tau &= \langle s(t)\rangle \\ &= \sum_A \int_{-\infty}^{\infty}\mathrm{d}f \int \mathrm{d}\widehat{\Omega}\,\langle \tilde{h}_A(f,\widehat{\Omega})\rangle \mathrm{e}^{-2\pi \mathrm{i} f t}\,\boldsymbol{D}(\widehat{\Omega},f):\boldsymbol{e}^A(\widehat{\Omega}) \\ &= 0.\end{aligned} \tag{B10}$$

Since the expectation value of $s(t)$ vanishes we need to consider higher moments such as $s^2(t)$. Using equations (6) and (B1) we find

$$\langle s^2(t)\rangle = \int_0^\infty \mathrm{d}f\, S_h(f)\mathcal{R}(f), \tag{B11}$$

where the transfer function $\mathcal{R}(f)$ is given by

$$\mathcal{R}(f) = \int \frac{\mathrm{d}\widehat{\Omega}}{4\pi}\sum_A F^A(\widehat{\Omega},f)F^A(\widehat{\Omega},f)^*, \tag{B12}$$

and $F^A(\widehat{\Omega},f) = \boldsymbol{D}(\widehat{\Omega},f):\boldsymbol{e}^A(\widehat{\Omega})$ is the detector response function. In the low-frequency limit, $f \ll f_*$, it is easy to show that $\mathcal{R}(f) = \frac{2}{5}\sin^2\beta$, where $\cos\beta = \boldsymbol{u}\cdot\boldsymbol{v}$ is the angle between the interferometer arms.

The response of the interferometer can be expressed in terms of the *strain spectral density*, $\tilde{h}_s(f)$, which has units of $\mathrm{Hz}^{-1/2}$ and is defined by

$$\langle s^2(t)\rangle = \int_0^\infty \mathrm{d}f\,\tilde{h}_s^2(f) = \int_0^\infty \mathrm{d}f\, S_h(f)\mathcal{R}(f). \tag{B13}$$

[7] The limit $\tau\to\infty$ is approximated in practice by observing for a period much longer than the period of the gravitational wave.

We see that the strain spectral density in the interferometer is related to the spectral density of the source by

$$\tilde{h}_s(f) = \sqrt{S_h(f)\mathcal{R}(f)}. \tag{B14}$$

The total output of the interferometer is given by the sum of the signal and the noise:

$$S(t) = s(t) + n(t). \tag{B15}$$

Assuming the noise is Gaussian, it can be fully characterized by the expectation values

$$\langle \tilde{n}(f) \rangle = 0, \qquad \text{and} \qquad \langle \tilde{n}^*(f)\tilde{n}(f') \rangle = \tfrac{1}{2}\delta(f - f')S_n(f), \tag{B16}$$

where $S_n(f)$ is the noise spectral density. The total noise power in the interferometer is thus

$$\langle n^2(t) \rangle = \int_0^\infty \mathrm{d}f\, S_n(f) = \int_0^\infty \mathrm{d}f\, \tilde{h}_n^2(f) \tag{B17}$$

where $\tilde{h}_n(f)$ is the strain spectral density due to the noise. Comparing equations (B13) and (B17), we define the signal-to-noise ratio at frequency f by

$$\mathrm{SNR}(f) = \frac{\tilde{h}_s^2(f)}{\tilde{h}_n^2(f)} = \frac{S_h(f)\mathcal{R}(f)}{S_n(f)}. \tag{B18}$$

Sensitivity curves for space-based interferometers typically display the effective strain noise

$$\tilde{h}_{\mathrm{eff}}(f) = \sqrt{\frac{S_n(f)}{\mathcal{R}(f)}}. \tag{B19}$$

At high frequencies it is the decay of the transfer function $\mathcal{R}(f)$ leads to a rise in the effective noise floor. The actual noise power, $S_n(f)$, does not rise significantly at high frequencies for space-based systems.

Appendix C. The LISA detector

Using the coordinate system shown in figure A1, the unit vectors along each arm are given by

$$\begin{aligned} \boldsymbol{u} &= \frac{1}{2}\hat{x} + \frac{\sqrt{3}}{2}\hat{y} \\ \boldsymbol{v} &= -\frac{1}{2}\hat{x} + \frac{\sqrt{3}}{2}\hat{y}, \end{aligned} \tag{C1}$$

and the gravitational wave is described by

$$\begin{aligned} \widetilde{\Omega} &= \cos\phi \sin\theta\, \hat{x} + \sin\phi \sin\theta\, \hat{y} + \cos\theta\, \hat{z} \\ \hat{m} &= \sin\phi\, \hat{x} - \cos\phi\, \hat{y} \\ \hat{n} &= \cos\phi \cos\theta\, \hat{x} + \sin\phi \cos\theta\, \hat{y} - \sin\theta\, \hat{z} \\ \boldsymbol{e}^+ &= \hat{m} \otimes \hat{m} - \hat{n} \otimes \hat{n} \\ \boldsymbol{e}^\times &= \hat{m} \otimes \hat{n} + \hat{n} \otimes \hat{m}. \end{aligned} \tag{C2}$$

The angle between the interferometer arms is $\arccos(\boldsymbol{u}\cdot\boldsymbol{v}) = \beta = \pi/3$. The various ingredients we need to calculate $\mathcal{R}(f)$ are

$$\boldsymbol{u} \cdot \widehat{\Omega} = \sin(\phi + \pi/6) \sin\theta \tag{C3}$$

$$\boldsymbol{v} \cdot \widehat{\Omega} = \sin(\phi - \pi/6) \sin\theta \tag{C4}$$

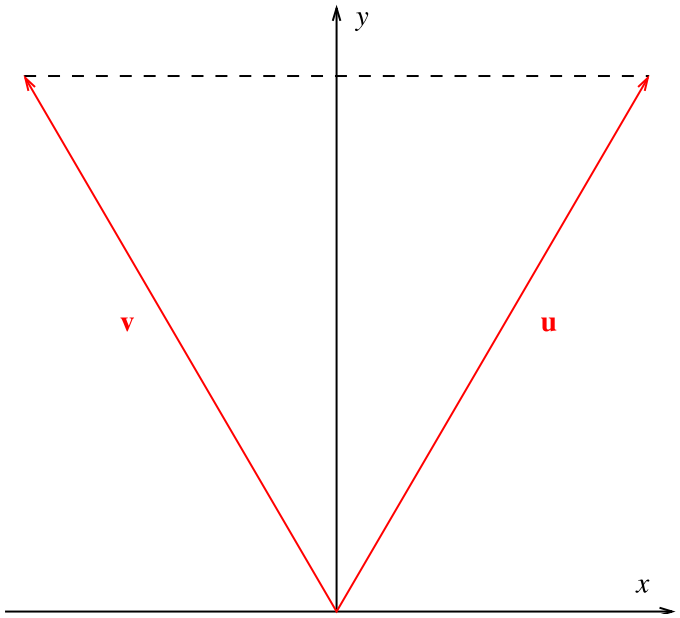

Figure A1. The coordinate system used to evaluate LISA's transfer function.

and

$$(\boldsymbol{u}\otimes\boldsymbol{u}):\boldsymbol{e}^{+}=\tfrac{1}{4}\sin^2\theta+\tfrac{1}{2}\cos^2\theta\cos^2\phi-\frac{\sqrt{3}}{4}\sin 2\phi\,(1+\cos^2\theta). \tag{C5}$$

$$(\boldsymbol{v}\otimes\boldsymbol{v}):\boldsymbol{e}^{+}=\tfrac{1}{4}\sin^2\theta+\tfrac{1}{2}\cos^2\theta\cos^2\phi+\frac{\sqrt{3}}{4}\sin 2\phi\,(1+\cos^2\theta). \tag{C6}$$

$$(\boldsymbol{u}\otimes\boldsymbol{u}):\boldsymbol{e}^{\times}=-\cos\theta\sin(2\phi+\pi/3). \tag{C7}$$

$$(\boldsymbol{v}\otimes\boldsymbol{v}):\boldsymbol{e}^{\times}=-\cos\theta\sin(2\phi-\pi/3). \tag{C8}$$

Before proceeding to find $\mathcal{R}(f)$ it is instructive to evaluate the detector response functions, $F^A(\widehat{\Omega},f)$, at zero frequency:

$$\begin{aligned}F^{+}(\widehat{\Omega})&=\tfrac{1}{2}(\boldsymbol{u}\otimes\boldsymbol{u}-\boldsymbol{v}\otimes\boldsymbol{v}):\boldsymbol{e}^{+}\\&=-\frac{\sqrt{3}}{4}\sin 2\phi\,(1+\cos^2\theta),\end{aligned} \tag{C9}$$

and

$$\begin{aligned}F^{\times}(\widehat{\Omega})&=\tfrac{1}{2}(\boldsymbol{u}\otimes\boldsymbol{u}-\boldsymbol{v}\otimes\boldsymbol{v}):\boldsymbol{e}^{\times}\\&=-\frac{\sqrt{3}}{2}\cos 2\phi\cos\theta.\end{aligned} \tag{C10}$$

Inserting equations (C3) through (C8) into equation (B12) gives the transfer function $\mathcal{R}(f)$ in terms of an integral over the angles θ and ϕ. Our explicit expression for LISA's transfer function agrees with that found by Larson *et al* [26] using an alternative approach.

We were unable to perform the angular integral to arrive at a general form for $\mathcal{R}(f)$, but for low frequencies the integrand can be expanded in a series to give

$$\mathcal{R}(f) = \frac{2}{5}\sin^2\beta\left(1 - \frac{37\cos^2(\beta/2) - 10\cos^4(\beta/2) - 1}{84\cos^2(\beta/2)}\left(\frac{f}{f_*}\right)^2 + \frac{20\cos^6(\beta/2) + 163\cos^2(\beta/2) - 80\cos^4(\beta/2) - 6}{2268\cos^2(\beta/2)}\left(\frac{f}{f_*}\right)^4 - \cdots\right). \quad \text{(C11)}$$

At frequencies above $f \sim \frac{3}{2}f_*$, the sinc function takes over and the transfer function falls of as $1/f^2$. Setting $\beta = \pi/3$, we find that a good approximation for the transfer function is given by

$$\mathcal{R}(f) = \begin{cases} \dfrac{3}{10}\left(1 - \dfrac{169}{504}\left(\dfrac{f}{f_*}\right)^2 + \dfrac{425}{9072}\left(\dfrac{f}{f_*}\right)^4 - \dfrac{165\,073}{47\,900\,160}\left(\dfrac{f}{f_*}\right)^6\right), & f < \frac{3}{2}f_* \\ \dfrac{16\,783\,143}{126\,156\,800}\left(\dfrac{3f_*}{2f}\right)^2, & f \geqslant \frac{3}{2}f_*. \end{cases} \quad \text{(C12)}$$

The coefficient in front of the high-frequency term is chosen so that the transfer function is continuous at $f = \frac{3}{2}f_*$.

Now that we have calculated the transfer function, our next task is to estimate the detector noise power, $S_n(f)$. There are many noise contributions discussed in the LISA pre-phase A report [8]. The dominant ones are thought to be acceleration noise from the inertial sensors and position noise due to laser shot noise. A position noise of $\widetilde{\delta x} = 2 \times 10^{-11}$ m Hz$^{-1/2}$ is quoted for each LISA spacecraft. There are two such contributions per arm, giving a total of four contributions for the interferometer. Since the contributions are uncorrelated they add in quadrature to give a total position noise of $2\widetilde{\delta x}$. Dividing this by the optical path length of $2L$ and squaring gives the position noise power:

$$S_n^{\rm pos}(f) = \left(\frac{\widetilde{\delta x}}{L}\right)^2. \quad \text{(C13)}$$

An acceleration noise of $\widetilde{\delta a} = 3 \times 10^{-15}$ m s^{-2} Hz$^{-1/2}$ is quoted for each inertial sensor. This noise acts coherently on the incoming and outgoing signal, for a combined acceleration noise of $2\widetilde{\delta a}$ per spacecraft. There are four such contributions in the interferometer that add in quadrature for a total acceleration noise of $4\widetilde{\delta a}$. Dividing this by the square of the angular frequency of the gravitational wave yields the effective position noise due to spurious accelerations. Dividing the effective position noise by the optical path length and squaring gives the acceleration noise power:

$$S_n^{\rm accl}(f) = \left(\frac{2\widetilde{\delta a}}{(2\pi f)^2 L}\right)^2. \quad \text{(C14)}$$

Adding together the acceleration and position noise power gives the total noise power. Using the nominal values for the LISA mission [8] we obtain

$$S_n(f) = \left(9.24 \times 10^{-40}\left(\frac{\rm mHz}{f}\right)^4 + 1.6 \times 10^{-41}\right)\ {\rm Hz}^{-1}. \quad \text{(C15)}$$

Inserting the above expression for $S_n(f)$, along with the approximate expression for the transfer function (C12), into equation (B19) yields a useful analytic approximation for the effective

strain noise, $\tilde{h}_{\rm eff}(f)$, in the LISA interferometer. The analytic approximation is compared with the full numerical result in figure 3.

LISA reaches a peak sensitivity in the frequency range $3 \times 10^{-3} \rightarrow 10^{-2}$ Hz. Using equations (B18) and (B19) we have

$$S_h(f) = \tilde{h}^2_{\rm eff}(f)\,{\rm SNR}(f). \tag{C16}$$

For a SNR of 2, this translates into a sensitivity of

$$\tilde{h}_{\rm eff}(f) = 6.2 \times 10^{-21} \left(\frac{\Omega_{\rm gw}(f)h_0^2}{10^{-13}}\right)^{1/2} \left(\frac{f}{\rm mHz}\right)^{3/2} {\rm Hz}^{-1/2}. \tag{C17}$$

Thus, a stochastic background with $\Omega_{\rm gw}(f)h_0^2 > 7\times10^{-12}$ should dominate LISA's instrument noise for frequencies near 3 mHz. The difficulty would come in deciding if the interferometer response was due to instrument noise or a stochastic background, as both are Gaussian random processes. One way to be sure is to fly two LISA interferometers and cross-correlate their outputs.

Appendix D. Cross-correlation

The cross-correlation of two interferometers can be expressed in the Fourier domain:

$$C \simeq \int_{-\infty}^{\infty} {\rm d}f \int_{-\infty}^{\infty} {\rm d}f'\, \delta_T(f - f')\tilde{S}_1^*(f)\tilde{S}_2(f')\widetilde{Q}(f'). \tag{D1}$$

The strain amplitude in the ith detector,

$$S_i(f) = h_i^{\rm astro}(f) + s_i(f) + n_i(f), \tag{D2}$$

has contributions from resolvable astrophysical sources $h_i^{\rm astro}$, the stochastic background s_i, and intrinsic detector noise n_i. The function δ_T that appears in the Fourier space version of the correlation function is the 'finite-time delta function'

$$\delta_T = \int_{-T/2}^{T/2} {\rm d}t\, {\rm e}^{-2\pi {\rm i} f t} = \frac{\sin(\pi f T)}{\pi f}. \tag{D3}$$

It obeys

$$\delta_T(0) = T \qquad \text{and} \qquad \delta(x) = \lim_{T\rightarrow\infty} \delta_T(x). \tag{D4}$$

After removing resolvable astrophysical sources[8], the ensemble average of C is given by

$$\langle C\rangle = \langle s_1, s_2\rangle + \langle s_1, n_2\rangle + \langle n_1, s_2\rangle + \langle n_1, n_2\rangle = \langle s_1, s_2\rangle. \tag{D5}$$

Note that terms involving the noise vanish as the noise is uncorrelated to the signal, and the noise in different detectors is also uncorrelated. Thus,

$$\langle C\rangle = \langle s_1, s_2\rangle = \int_{-\infty}^{\infty} {\rm d}f \int_{-\infty}^{\infty} {\rm d}f'\, \delta_T(f - f')\langle\tilde{s}_1^*(f)\tilde{s}_2(f')\rangle\, \widetilde{Q}(f'). \tag{D6}$$

[8] For bright sources it is possible to use the Doppler modulation and the sweep of the antenna patterns to accurately identify the gravitational waveform. The contribution of these point sources can then be removed from the time series $S(t)$. The subtraction is not perfect, and a small residual will remain. The residuals form part of the confusion-limited astrophysical foreground.

Our next task is to evaluate the quantity $\langle \tilde{s}_1^*(f)\tilde{s}_2(f')\rangle$ that appears in equation (D6). Taking the Fourier transform of the expression in (6) and performing the ensemble average we find

$$\langle \tilde{s}_1^*(f)\tilde{s}_2(f')\rangle = \tfrac{1}{2}\delta(f-f')S_h(f)\,\gamma(f)\,\tfrac{2}{5}\sin^2\beta, \tag{D7}$$

where $\gamma(f)$ is the overlap reduction function

$$\gamma(f) = \frac{5}{2\sin^2\beta}\int \frac{\mathrm{d}\widehat{\Omega}}{4\pi}\left(F_1^{+*}(\widehat{\Omega},f)F_2^{+}(\widehat{\Omega},f) + F_1^{\times *}(\widehat{\Omega},f)F_2^{\times}(\widehat{\Omega},f)\right)\mathrm{e}^{-2\pi \mathrm{i} f\widehat{\Omega}\cdot(\boldsymbol{x}_1-\boldsymbol{x}_2)/c}. \tag{D8}$$

The normalization is chosen so that $\gamma(0) = 1$. The function $\gamma(f)$ is Hermitian in the sense that $\gamma_{12}(f) = \gamma_{21}^*(f)$. The inverse Fourier transform of $\gamma(f)$ is a real function since $\gamma^*(f) = \gamma(-f)$. Inserting equation (D7) into equation (D6) yields the expectation value of C:

$$\langle C\rangle = \frac{T}{5}\sin^2\beta\int_{-\infty}^{\infty}\mathrm{d}f\, S_h(f)\gamma(f)\widetilde{Q}(f). \tag{D9}$$

The noise in a measurement of C is given by $N = C - \langle C\rangle$, and the signal-to-noise ratio (squared) is given by

$$\mathrm{SNR}^2 \equiv \frac{\langle C\rangle^2}{\langle N^2\rangle} = \frac{\langle C\rangle^2}{\langle C^2\rangle - \langle C\rangle^2}. \tag{D10}$$

Our task is to find the filter function $\widetilde{Q}(f)$ that maximizes this signal-to-noise ratio. A lengthy but straightforward calculation yields

$$\langle N^2\rangle = \frac{T}{4}\int_{-\infty}^{\infty}|\widetilde{Q}(f)|^2 M(f)\,\mathrm{d}f \tag{D11}$$

where

$$M(f) = S_{n1}(f)\,S_{n2}(f) + S_{n1}(f)S_h(f)\mathcal{R}_2(f) + S_{n2}(f)S_h(f)\mathcal{R}_1(f) + S_h^2(f)\left(\tfrac{4}{25}\sin^4\beta\,|\gamma(f)|^2 + \mathcal{R}_1(f)\mathcal{R}_2(f)\right). \tag{D12}$$

Here $S_{n,i}$ and $\mathcal{R}_i$ denote the spectral noise and the transfer function for the ith interferometer. The square of the signal-to-noise ratio can be written as

$$\mathrm{SNR}^2 = \frac{4T}{25}\sin^4\beta\,\frac{\{\widetilde{P},\widetilde{Q}\}^2}{\{\widetilde{Q},\widetilde{Q}\}}, \tag{D13}$$

where $\{A, B\}$ denotes the inner product [17]

$$\{A,B\} = \int_{-\infty}^{\infty}\mathrm{d}f\, A^*(f)B(f)M(f), \tag{D14}$$

and

$$\widetilde{P}(f) = \frac{S_h(f)\gamma^*(f)}{M(f)}. \tag{D15}$$

The signal-to-noise ratio is maximized by choosing the optimal filter 'parallel' to $\widetilde{P}$. Since the normalization of $\widetilde{Q}$ drops out, we set $\widetilde{Q}(f) = \widetilde{P}(f)$ [16, 17]. Using this filter, the optimal signal-to-noise ratio for the cross correlated interferometers is given by

$$\mathrm{SNR}^2 = \frac{8T}{25}\sin^4\beta\int_0^{\infty}\mathrm{d}f\,\frac{|\gamma(f)|^2 S_h^2(f)}{M(f)}, \tag{D16}$$

or, equivalently, as

$$\mathrm{SNR}^2 = \frac{9H_0^4\sin^4\beta}{50\pi^4}\,T\int_0^{\infty}\mathrm{d}f\,\frac{|\gamma(f)|^2\,\Omega_{\mathrm{gw}}^2(f)}{f^6 M(f)}. \tag{D17}$$

References

[1] de Bernardis P *et al* 2000 *Nature* **404** 955
[2] Balbi A *et al* 2000 *Astrophys. J.* **545** L1
[3] Bennett C L *et al* 1996 *Astrophys. J.* **464** L1
[4] Mather J C *et al* 1990 *Astrophys. J.* **354** L37
[5] Cornish N J and Larson S L 2001 in preparation
[6] Hogan C J 2000 *Phys. Rev. Lett.* **85** 2044
[7] Riazuelo A and Uzan J-P 2000 *Phys. Rev.* D **62** 083506
[8] Bender P L *et al* 1998 *LISA Pre-Phase A Report*
[9] Schneider R, Ferrara A, Ciardi B, Ferrari V and Matarrese S 2000 *Mon. Not. R. Astron. Soc.* **317** 365
Schneider R, Ferrari V, Matarrese S and Portegies Zwart S F 2001 *Mon. Not. R. Astron. Soc.* **324** 797
[10] Maggiore M 2000 *Phys. Rep.* **331** 283
[11] Krauss L and White M 1992 *Phys. Rev. Lett.* **69** 869
[12] Tinto M, Armstrong J W and Estabrook F B 2001 *Phys. Rev.* D **63** 021101(R)
[13] Hogan C J and Bender P L 2001 *Phys. Rev.* D to appear
(Hogan C J and Bender P L 2001 *Preprint* astro-ph/0104266)
[14] Michelson P F 1987 *Mon. Not. R. Astron. Soc.* **227** 933
[15] Christensen N 1992 *Phys. Rev.* D **46** 5250
[16] Flanagan E E 1993 *Phys. Rev.* D **48** 2389
[17] Allen B 1996 *Proc. Les Houches School on Astrophysical Sources of Gravitational Waves* ed J-A Marck and J-P Lasota (Cambridge: Cambridge University Press) p 373
[18] Allen B and Romano J D 1999 *Phys. Rev.* D **59** 102001
[19] Hellings R W 1983 *Gravitational Radiation* ed N Dereulle and T Piran (Amsterdam: North-Holland) p 485
[20] Ungarelli C and Vecchio A 2001 *Phys. Rev.* D **63** 064030
[21] Caldwell R R, Kamionkowski M and Wadley L 1999 *Phys. Rev.* D **59** 027101
[22] Boyle B J *et al* 1993 *Mon. Not. R. Astron. Soc.* **260** 49
[23] McHardy I M *et al* 1998 *Mon. Not. R. Astron. Soc.* **295** 641
[24] Schilling R 1997 *Class. Quantum Grav.* **14** 1513
[25] Armstrong J W, Estabrook F B and Tinto M 1999 *Astrophys. J.* **527** 814
[26] Larson S L, Hiscock W A and Hellings R W 2000 *Phys. Rev.* D **62** 062001